Proceedings of the Pakistan Academy of Sciences: B Life and Environmental Sciences 63(3): ------- (2026)
Copyright © Pakistan Academy of Sciences
ISSN (Print): 2518-4261; ISSN (Online): 2518-427X
http://doi.org/10.53560/PPASB(63-3)1141

Pakistan Academy of Sciences

Research Article

Morphological and Leaf-Epidermal Trait Variation among 21 Poaceae Species from Layyah District, Pakistan

Rafia Nawaz[1], Khafsa Malik[1*], Muhammad Imran[2*], Ubaidur Rahman[1], Najeeb Ullah[3], and Bushra Ali[3]

[1]Department of Botany, PMAS Arid Agriculture University, Rawalpindi, Punjab, Pakistan
[2]State Key Laboratory of Herbage Improvement and Grassland Agro-Ecosystems, College of Ecology, Lanzhou University, Lanzhou, 730000, China
[3]Department of plant Sciences, Quaid-i-Azam University, Islamabad, Pakistan

ACCEPTED MANUSCRIPT

Abstract: Poaceae is an ecologically dominant plant family, yet integrated morpho-anatomical assessments of grasses from the semi-arid plains of Pakistan remain limited. We aimed to (i) quantify morphological functional traits and leaf micromorphology of 21 Poaceae species from diverse habitats in Layyah District, Punjab, Pakistan, and (ii) identify the traits that contribute most to separating species and leaf surfaces. We quantified plant height, culm number, node number, internodal distance, and leaf dimensions. Stomatal and epidermal characteristics were examined using light microscopy and scanning electron microscopy (SEM). Trait variation among species was assessed via principal component analysis (PCA) and hierarchical clustering; anatomical variation was evaluated using stomatal and epidermal trait-based PCA. For the 19 species with complete morphological data, the first two PCA axes explained 78.6% of total variation (PC1 = 62.6%, PC2 = 16.0%) and reflected mainly plant size and leaf dimensions. Hierarchical clustering separated four large grasses from 15 smaller species (mean silhouette width = 0.54). Anatomical PCA explained 90.05% of total variation (PC1 = 70.21%, PC2 = 19.84%), with stomatal traits contributing most to species separation. Adaxial and abaxial leaf surfaces differed significantly (paired tests and PERMANOVA restricted within species; $p \leq 0.001$). SEM revealed modified stomata, dense trichomes, thick cuticles, silica bodies, and other epidermal features that are commonly associated with drought resistance in grasses. These results document distinct combinations of morphological and leaf-epidermal traits among grasses of Layyah District and provide a baseline for future studies that test trait–environment relationships with measured habitat variables and physiological data.

Keywords: Poaceae, Functional Traits, Leaf Micromorphology, Stomatal Architecture, Epidermal Traits, Scanning Electron Microscopy, Arid Ecosystems.

1. INTRODUCTION

The Poaceae family, comprising more than 12,000 species and over 780 genera, represents one of the most ecologically and economically significant plant lineages worldwide, occupying diverse habitats ranging from grasslands, savannas, and wetlands to arid deserts and alpine ecosystems [1, 2]. Poaceae species contribute substantially to ecosystem functioning by maintaining vegetation structure, supporting biodiversity, stabilizing soils, and regulating terrestrial carbon dynamics [3]. Their evolutionary success is largely associated with remarkable physiological and structural adaptations, particularly the widespread evolution of C_4 photosynthesis, which enhances carbon assimilation and resource-use efficiency under warm and water-limited conditions [4, 5]. In addition, anatomical modifications such as Kranz anatomy, specialized stomatal structures, and efficient epidermal arrangements enable many grasses to tolerate drought and high-temperature environments [6]. Beyond their ecological significance, Poaceae species provide essential

Received: August 2026; Revised: September 2026; Accepted: September 2026
* Corresponding Author: Khafsa Malik and Muhammad Imran < khafsamalik786@gmail.com; muhammad2025@lzu.edu.cn >

ecosystem services through soil stabilization, erosion control, and nutrient cycling. Extensive root systems and rhizomatous growth forms improve soil structure and contribute to ecosystem resilience by reducing degradation processes [7]. Furthermore, grasses play a crucial role in global carbon sequestration through accumulation of above- and belowground biomass [8]. Their dominance in natural ecosystems and human-modified landscapes highlights their importance as ecological engineers, habitat providers, and forage resources [9, 10]. However, dense growth and competitive abilities of some Poaceae species may also create management challenges in agricultural and natural systems [11].

Poaceae is also fundamental to global food security, with economically important species, including maize (*Zea mays*), rice (*Oryza sativa*), wheat (*Triticum aestivum*), and sorghum (*Sorghum bicolor*), contributing substantially to human nutrition and the global caloric supply [3, 12]. In addition to their nutritional importance, grasses support livestock production by providing essential fodder resources and sustaining pastoral agricultural systems [13]. Several non-food applications further demonstrate their versatility; for example, *Arundo donax* is utilized for reed and paper production, whereas *Cortaderia selloana* is widely cultivated as an ornamental species [14]. In Pakistan, Poaceae species contribute significantly to agroecosystem stability by reducing soil erosion and supporting wheat- and rice-based agricultural landscapes [3, 11].

Despite their importance, accurate identification and ecological characterization of Poaceae species remain challenging due to high phenotypic plasticity and considerable overlap in external morphological characteristics [4]. Consequently, traditional morphological approaches alone are often insufficient for resolving species-level differences, highlighting the importance of detailed anatomical and micromorphological investigations [15, 16]. Leaf epidermal traits, including stomatal architecture, trichome density, and silica body characteristics, provide valuable taxonomic and functional information for distinguishing species and understanding ecological adaptation mechanisms [17, 18]. Particularly, stomatal size, density, and distribution influence plant responses to drought, light availability, and herbivory pressure by regulating gas exchange and water loss [19].

Advanced imaging approaches, especially scanning electron microscopy (SEM), provide detailed visualization of epidermal and stomatal structures that cannot be accurately resolved through conventional microscopy. SEM-based investigations facilitate precise assessment of stomatal morphology, trichome development, cuticular structures, and other diagnostic traits while providing insights into plant–environment interactions [20, 21]. Such anatomical approaches are particularly valuable in environmentally stressful regions where structural modifications determine plant persistence and ecological success.

Arid and semi-arid regions represent important natural laboratories for investigating plant adaptive strategies because vegetation is continuously exposed to water scarcity, temperature extremes, and soil-related limitations [22]. Native grasses inhabiting these environments have evolved diverse structural mechanisms, including sunken stomata, thick cuticles, silica deposition, and trichome development, which reduce water loss and enhance stress tolerance [23, 24]. Variations in leaf size, shape, and epidermal organization further contribute to optimizing water conservation and photosynthetic efficiency under fluctuating environmental conditions [18, 25].

These patterns apply directly to Pakistan, where much of the land is arid or semi-arid and native and cultivated grasses support rangeland grazing, soil conservation, and cereal-based farming [3, 11]. The Layyah District of Punjab, Pakistan, provides an ideal system for investigating these adaptations because it encompasses heterogeneous habitats, including semi-arid deserts, sandy rangelands, floodplain environments, and irrigated agricultural landscapes. Variation in vegetation structure, soil characteristics, and moisture availability across these habitats generates diverse selective pressures that may shape functional trait differentiation among Poaceae species [26, 27]. Understanding these trait responses can improve knowledge of grass adaptation to drought, soil erosion, and other environmental constraints [28].

Although previous studies have investigated Poaceae micromorphological traits [20, 29], integrated assessments combining taxonomy, functional morphology, anatomy, and ecological adaptation remain limited in Pakistan, particularly

ACCEPTED MANUSCRIPT

in arid and semi-arid ecosystems [3, 30, 31]. The application of advanced techniques, such as SEM, remains largely unexplored in native grasses of southern Punjab, thereby restricting our understanding of their adaptive mechanisms. This study therefore addressed three questions: (1) how strongly do 21 Poaceae species from Layyah District differ in plant architecture and leaf dimensions, and do they form distinct morphological groups? (2) How do stomatal and epidermal traits, including stomatal index (SI) and trichome index (TI), vary among species and between the adaxial and abaxial leaf surfaces? (3) Which traits contribute most to separating species? We expected species to separate mainly along a plant-size axis and stomatal traits to differ strongly between leaf surfaces. Because environmental variables were not measured, the study is descriptive and comparative: it documents trait variation that can generate hypotheses about adaptation to water-limited conditions but does not test them.

2. MATERIALS AND METHODS

2.1. Study Area and Sampling Period

The study was conducted from May 2024 to June 2025 in Layyah District, Punjab, Pakistan, an ecologically diverse region characterized by arid and semi-arid climatic conditions and heterogeneous grass habitats. The primary sampling site was Bakhry Ahmed Khan (30.7531° N, 70.8655° E), selected due to its representative Poaceae diversity; however, additional specimens were collected from different ecological zones across the district to encompass habitat variability. The region experiences a hot semi-arid climate, with mean annual temperatures ranging from approximately 26 °C to summer maxima of 40-45 °C, while annual precipitation averages around 439 mm, primarily concentrated during the monsoon season [32]. The combination of high temperature, irregular rainfall, and variable soil moisture availability creates strong environmental pressures that influence plant structural and anatomical adaptations, making Layyah an appropriate location for investigating drought-related functional traits in grasses. The sampled habitats included sandy desert rangelands (Thal-type dunes and sand plains), irrigated agricultural fields, floodplain loamy soils near river systems, and semi-arid grass-shrub communities. These habitats represented contrasting environmental conditions in terms of vegetation density, soil texture, and water availability. Because Poaceae species differ in their reproductive phenology, each species was sampled during its own peak flowering period (Table 1). The 13-month sampling window therefore reflects staggered species-specific sampling rather than repeated seasonal sampling of the same species. Nevertheless, seasonal variation in leaf traits, including stomatal density, may have contributed to the observed interspecific differences.

2.2. Plant Material Collection and Identification

A total of 21 Poaceae species representing 20 genera were collected during their respective flowering periods from different ecological habitats within Layyah District (Table 1). Apart from the three crops (*Oryza sativa*, *Zea mays*, and *Sorghum bicolor*), which were sampled from farmers' fields, all species, including those of temperate origin such as *Agrostis stolonifera*, *Lolium perenne*, *Phleum pratense*, and *Bouteloua dactyloides*, were collected from naturally growing populations in the sampled habitats rather than from cultivated or experimental plots. Most specimens were collected at Bakhri Ahmed Khan (30.7531° N, 70.8655° E), with additional specimens from other locations in the district covering the four habitat types described in Section 2.1. The habitat of each specimen was not recorded systematically at the species level, so traits were compared among species but not among habitat types. Sampling was conducted randomly to capture interspecific morphological and anatomical variation associated with contrasting environmental conditions. For each species, mature and healthy individuals were selected for morphological measurements and anatomical investigations. Plant specimens were identified using standard taxonomic references, including the Flora of Pakistan and the International Plant Name Index (IPNI) databases. Voucher specimens were prepared and deposited in the herbarium for future reference. The collected species represented diverse ecological and functional groups, including perennial grasses, annual grasses, forage species, and economically important crops. The flowering period of each species was recorded to ensure accurate identification based on both vegetative and reproductive characteristics and to optimize sampling during peak physiological activity.

ACCEPTED MANUSCRIPT

Table 1. Taxonomic diversity and flowering periods of 21 Poaceae species collected from different ecological habitats of Layyah District, Punjab, Pakistan.

S. No.	Scientific Name	Common Name	Flowering Season
1	*Agrostis stolonifera*	Creeping bentgrass	July to August
2	*Alopecurus myosuroides*	Blackgrass	May to August
3	*Arundo donax*	Giant reed	June to December
4	*Bouteloua dactyloides*	Buffalo grass	June to August
5	*Chloris gayana*	Rhodes grass	August to September
6	*Chrysopogon zizanioides*	Vetiver grass	August to October
7	*Cortaderia selloana*	Pampas grass	August to October
8	*Dactyloctenium aegyptium*	Crowfoot grass	July to October
9	*Digitaria sanguinalis*	Crabgrass	July to September
10	*Echinochloa crus-galli*	Barnyard grass	June to October
11	*Eleusine indica*	Goosegrass	June to August
12	*Eragrostis pilosa*	Lovegrass	May to September
13	*Lolium perenne*	Perennial ryegrass	May to July
14	*Oryza sativa*	Rice	July to October
15	*Panicum virgatum*	Switchgrass	July to September
16	*Phleum pratense*	Timothy grass	June to August
17	*Schizachyrium maritimum*	Gulf bluestem	July to September
18	*Sorghum bicolor*	Grain sorghum	March to June
19	*Sorghum halepense*	Johnson grass	May to October
20	*Thysanolaena maxima*	Tiger grass / Broom grass	March to June
21	*Zea mays*	Maize / Corn	March to April

ACCEPTED MANUSCRIPT

2.3. Morphological Trait Characterization

Morphological functional traits were recorded for all collected species, including plant height (cm), number of culms, number of nodes, internodal distance (cm), leaf length (cm), leaf width (cm), leaf sheath characteristics, and leaf pubescence. Measurements were obtained from three mature individuals per species, with each trait measured three to five times per individual. Repeated measurements on the same individual were averaged, and the three individuals per species were treated as the biological replicates. Mean values and standard errors (SE) were calculated to summarize trait variation among species. These traits were selected because they represent major components of plant architecture, biomass allocation, and resource acquisition strategies. Quantitative morphological measurements were subsequently used for functional trait analysis through multivariate approaches.

2.4. Light Microscopy and Epidermal Preparation

Leaf epidermal characteristics were examined following a modified protocol of Cotton [33]. Mature, fully expanded leaves were collected from three individuals per species and maintained in distilled water for two hours to preserve tissue hydration. Epidermal impressions were prepared using the nail-polish replica technique and epidermal peeling where required. Samples were fixed in FAA solution (formalin: acetic acid: alcohol, 1:1:3) and preserved in 70% ethanol. Suberin-associated structures were examined using Sudan IV staining, while epidermal preparations were stained with Delafield's haematoxylin and mounted using glycerin jelly [34, 35]. Microscopic observations were performed using a Nikon ECLIPSE E200 compound microscope equipped with a DCM35 digital camera. Observations were conducted at different magnifications to evaluate

stomatal morphology, epidermal cell characteristics, and trichome presence. Anatomical terminology followed Metcalfe [36, 37].

2.5. Scanning Electron Microscopy (SEM) Analysis

We conducted detailed micromorphological investigations using scanning electron microscopy. Mature, undamaged leaf segments were collected from the middle portion of leaves from three individuals per species. Two leaves per individual were examined to capture within-species variation. Where epicuticular wax accumulation was present, samples were treated with xylene for 12-24 hours to remove surface wax while maintaining epidermal integrity. We mounted prepared samples on aluminium stubs with double-sided adhesive tape, positioned them according to leaf surface orientation, and coated them with gold-palladium [38-40]. Samples were examined using a JEOL JSM-5910 scanning electron microscope at the Central Resource Laboratory. SEM images were used to characterize stomatal morphology, epidermal ornamentation, silica structures, papillae, trichomes, hooks, and surface patterns.

2.6. Statistical and Functional Trait Analysis

Quantitative morphological and anatomical data were analyzed using multivariate statistical approaches to evaluate functional differentiation among Poaceae species. Six morphological functional traits, including plant height, number of culms, number of nodes, internodal distance, leaf length, and leaf width, were standardized using z-score transformation before principal component analysis (PCA). For *Sorghum halepense* and *Thysanolaena maxima*, culms were too numerous to count reliably, and nodes and internodes could not be measured on the dense clumps (Table 2). Because these values were not measured, the two species were excluded from the morphological PCA and clustering (n = 19); their morphology is described in Table 2 in Section 3.1. PCA was performed using the FactoMineR package in R to identify major axes of morphological trait variation. Species scores, trait loadings, eigenvalues, and trait contributions were extracted to determine the variables responsible for species separation, and PCA ordinations were visualized using customized biplots generated with ggplot2 and ggrepel.

Functional similarity among the 19 species was assessed using hierarchical cluster analysis based on the six standardized morphological traits. Euclidean distance matrices were calculated from scaled trait values, followed by Ward's minimum variance clustering (Ward.D2). The optimal number of functional groups was determined using mean silhouette width analysis, which evaluates within-cluster cohesion and between-cluster separation. Stomatal and epidermal anatomical variation was evaluated using PCA based on seven leaf functional traits, including stomatal length, stomatal width, stomatal density, epidermal cell density, trichome density, stomatal index (SI), and trichome index (TI). Both PCAs used mean values: species means for the morphological PCA (n = 19) and species-by-surface means for the anatomical PCA (n = 42). Within-species variation is reported as SE in Tables 2 and 3 but was not part of the ordinations. The two PCAs contain different numbers of traits (six and seven) because they describe separate trait sets measured at different scales (whole plant and leaf epidermis) and were analyzed independently. Since some anatomical variables contained zero values due to the absence of stomata or trichomes on specific leaf surfaces, data were transformed using log(x + 1) and subsequently standardized before PCA. Trait contributions, $\cos^2$ values, and eigenvalues were calculated to identify the anatomical traits driving major patterns of variation. Because the adaxial and abaxial surfaces of each species are paired observations, surface differences were tested with paired t-tests on species PC1 and PC2 scores and with PERMANOVA (Euclidean distance, 999 permutations) in which permutations were restricted within species (adonis2 function of the R package *vegan*, with permutations restricted within species). Homogeneity of multivariate dispersion between surfaces was checked with PERMDISP (betadisper function of the R package *vegan*), because PERMANOVA results can be affected by unequal dispersion. Euclidean distance was retained because all traits were continuous and had been log-transformed (anatomical traits) and z-standardized, so that each trait contributed equally and the distance matrix matched the PCA ordination space; Bray–Curtis distance is intended for non-negative abundance data and Gower distance for mixed qualitative–quantitative data, neither of which applied to the trait matrices analyzed here.

ACCEPTED MANUSCRIPT

Descriptive statistics, including mean values and standard errors (SE), were calculated for all morphological and anatomical traits. Stomatal index (SI) and trichome index (TI) were calculated by following the method of Hadi *et al.* [38]:

$$SI = \frac{S}{E + S} \times 100 \quad (1)$$

$$TI = \frac{T}{E + T} \times 100 \quad (2)$$

where S represents the number of stomata, T represents the number of trichomes, and E represents the number of epidermal cells. All analyses were performed to quantify functional trait variation and identify morphological and anatomical strategies associated with the adaptation of Poaceae species to arid and semi-arid environments.

3. RESULTS AND DISCUSSION

3.1. Morphological Diversity and Functional Variation among Poaceae Species

A total of 21 Poaceae species were collected, mainly from Bakhri Ahmed Khan (30.7531° N, 70.8655° E), Layyah District, Punjab, Pakistan, representing diverse grass habitats. Morphological characterization revealed considerable variation among species in plant height, culm production, number of nodes, internodal distance, and leaf dimensions (Table 2). Plant stature showed the greatest variation among species, with *Arundo donax* exhibiting the highest plant height (450 ± 200 cm), whereas *Bouteloua dactyloides* represented the smallest growth form (12.5 ± 7.5 cm). Similarly, *Arundo donax* showed the highest number of culms (55 ± 40) and nodes (18 ± 7), contrasting with species such as *Zea mays* (3 ± 1 culms) and *Lolium perenne* (5.5 ± 1.5 culms). Internodal distance also varied markedly, with the maximum value recorded in *Cortaderia selloana* (19 ± 10 cm), while shorter internodes were observed in *Bouteloua dactyloides* (4 ± 2 cm) and *Dactyloctenium aegyptium* (5.5 ± 1.5 cm). Leaf morphology displayed pronounced interspecific differences. *Zea mays* possessed the largest leaves (70 ± 25 × 8 ± 2 cm), whereas *Agrostis stolonifera* exhibited considerably smaller leaves (8 ± 6 × 0.35 ± 0.15 cm). Qualitative morphological traits also varied among taxa, including leaf sheath structure and pubescence. Keeled leaf sheaths were observed in *Chloris gayana*, *Chrysopogon zizanioides*, *Dactyloctenium aegyptium*, and *Digitaria sanguinalis*, whereas leaf surface texture ranged from glabrous to scabrous, with *Cortaderia selloana* showing strongly roughened leaves. *Sorghum halepense* and *Thysanolaena maxima* formed dense clumps with culms too numerous to count, so their node number and internodal distance could not be measured; both were tall (215 ± 125 and 300 ± 150 cm) and had broad leaves (3.5 ± 1.5 and 3.9 ± 1.3 cm wide).

3.2. Functional Trait Differentiation among Poaceae Species Based on PCA

Principal component analysis of the six morphological traits for the 19 species with complete data showed strong differentiation among species. The first two principal components explained 78.6% of total variation, with PC1 accounting for 62.6% and PC2 for 16.0% (Figure 1). PC1 was a plant-size gradient, with the largest contributions from plant height (25.1%), node number (20.7%), leaf width (16.8%), internodal distance (15.0%), and leaf length (14.8%). Large species, including *Arundo donax*, *Cortaderia selloana*, *Zea mays*, *Sorghum bicolor*, and *Chrysopogon zizanioides*, had high positive PC1 scores, whereas smaller species, including *Bouteloua dactyloides*, *Agrostis stolonifera*, *Dactyloctenium aegyptium*, and *Eleusine indica*, had negative scores. PC2 contrasted culm number (39.8%) and node number (11.1%) with internodal distance (28.1%) and leaf length (19.9%). *Cortaderia selloana*, *Panicum virgatum*, and *Phleum pratense* had long internodes and leaves relative to culm production, whereas *Arundo donax*, *Bouteloua dactyloides*, and *Eragrostis pilosa* produced many culms.

3.3. Functional Trait Syndromes Revealed by Hierarchical Clustering

Hierarchical clustering of the 19 species identified two groups (Figure 2). Mean silhouette width was highest for k = 2 (0.54), compared with 0.51 for k = 3 and 0.52 for k = 4. The first group comprised four large grasses, *Arundo donax*, *Cortaderia selloana*, *Sorghum bicolor*, and *Zea mays*, characterized by tall stature and large leaves. The second group contained the remaining 15 species, which were smaller and had shorter internodes and smaller leaves. At k = 3, *Arundo donax* separated from the other large grasses because of its exceptional height and culm number.

ACCEPTED MANUSCRIPT

Table 2. Morphological trait variation among 21 Poaceae species collected from Layyah District, Punjab, Pakistan. Quantitative traits include plant height, culm number, node number, internodal distance, and leaf dimensions, while qualitative traits represent leaf sheath characteristics and leaf pubescence. Values are mean ± SE (n = 3 individuals per species); "Numerous" indicates culms too many to count reliably, and "–" indicates traits that could not be measured. These two species were therefore excluded from the multivariate morphological analyses.

No.	Plant Specimen	Plant Height (cm)	No. of Culms	No. of Nodes	Internodal Distance (cm)	Leaf Length × Width (cm)	Leaf Sheath Characteristics	Pubescence of Leaves
1	*Agrostis stolonifera*	37.5 ± 27.5	17 ± 8	4 ± 2	7.5 ± 4.5	8 ± 6 × 0.35 ± 0.15	Split, membranous	Glabrous
2	*Alopecurus myosuroides*	50 ± 25	6.5 ± 2.5	4.5 ± 1.5	9 ± 5	11.5 ± 7.5 × 0.4 ± 0.2	Rounded, smooth	Glabrous
3	*Arundo donax*	450 ± 200	55 ± 40	18 ± 7	19 ± 10	40 ± 15 × 5.5 ± 2.5	Persistent, glaucous	Glabrous
4	*Bouteloua dactyloides*	12.5 ± 7.5	22.5 ± 12.5	4 ± 1	4 ± 2	9.5 ± 6.5 × 0.3 ± 0.1	Flat, hairy	Ciliate
5	*Chloris gayana*	90 ± 50	10.5 ± 4.5	4 ± 2	10 ± 6	18 ± 7 × 0.65 ± 0.25	Compressed, keeled	Glabrous
6	*Chrysopogon zizanioides*	140 ± 50	30 ± 15	8.5 ± 2.5	17 ± 6	60 ± 35 × 1 ± 0.6	Overlapping, keeled	Glabrous
7	*Cortaderia selloana*	245 ± 55	35 ± 10	6.5 ± 2.5	25 ± 10	140 ± 50 × 1.7 ± 0.5	Tough, sharp-edged	Scabrous
8	*Dactyloctenium aegyptium*	37.5 ± 27.5	13.5 ± 8.5	5.5 ± 1.5	5.5 ± 1.5	8 ± 6 × 0.5 ± 0.2	Keeled, hairy at the mouth	Ciliate margins
9	*Digitaria sanguinalis*	45 ± 35	10.5 ± 4.5	5 ± 1	7.5 ± 3.5	8 ± 6 × 0.7 ± 0.3	Keeled, hairy	Pubescent
10	*Echinochloa crus-galli*	107.5 ± 52.5	5.5 ± 3.5	4 ± 2	16 ± 5	20 ± 15 × 1.2 ± 0.6	Compressed, glabrous	Glabrous
11	*Eleusine indica*	45 ± 35	10.5 ± 4.5	4 ± 2	7.5 ± 4.5	15 ± 10 × 0.65 ± 0.25	Flattened, ciliate	Sparsely hairy
12	*Eragrostis pilosa*	67.5 ± 42.5	27 ± 18	5 ± 2	10 ± 4	15 ± 10 × 0.35 ± 0.15	Split, hairy at the throat	Pilose
13	*Lolium perenne*	67.5 ± 42.5	5.5 ± 1.5	6.5 ± 1.5	11 ± 5	12.5 ± 7.5 × 0.4 ± 0.1	Closed, smooth	Glabrous
14	*Oryza sativa*	130 ± 40	15 ± 10	5.5 ± 1.5	20.5 ± 4.5	30 ± 15 × 1.9 ± 0.7	Tight, glabrous	Glabrous
15	*Panicum virgatum*	165 ± 75	4 ± 2	6.5 ± 2.5	23 ± 7	35 ± 20 × 1 ± 0.4	Open, smooth	Glabrous
16	*Phleum pratense*	95 ± 45	4 ± 2	5 ± 2	16.5 ± 5.5	22.5 ± 17.5 × 0.7 ± 0.3	Cylindrical, smooth	Glabrous
17	*Schizachyrium maritimum*	90 ± 50	10.5 ± 4.5	6 ± 3	14 ± 5	20 ± 15 × 0.5 ± 0.2	Tight, striate	Glabrous
18	*Sorghum bicolor*	230 ± 120	4 ± 2	11 ± 5	16.5 ± 7.5	60 ± 35 × 5 ± 2.5	Open, waxy bloom	Glabrous
19	*Sorghum halepense*	215 ± 125	Numerous	-	-	40 ± 25 × 3.5 ± 1.5	Glabrous to pubescent, ciliate	Blades glabrous; margins/midrib scabrous
20	*Thysanolaena maxima*	300 ± 150	Numerous	-	-	30 ± 15 × 3.9 ± 1.3	Glabrous or pilose at base	Blades glabrous or sparsely hairy
21	*Zea mays*	215 ± 75	3 ± 1	11.5 ± 4.5	16.5 ± 7.5	70 ± 25 × 8 ± 2	Tubular, hairy	Scabrous margins

ACCEPTED MANUSCRIPT

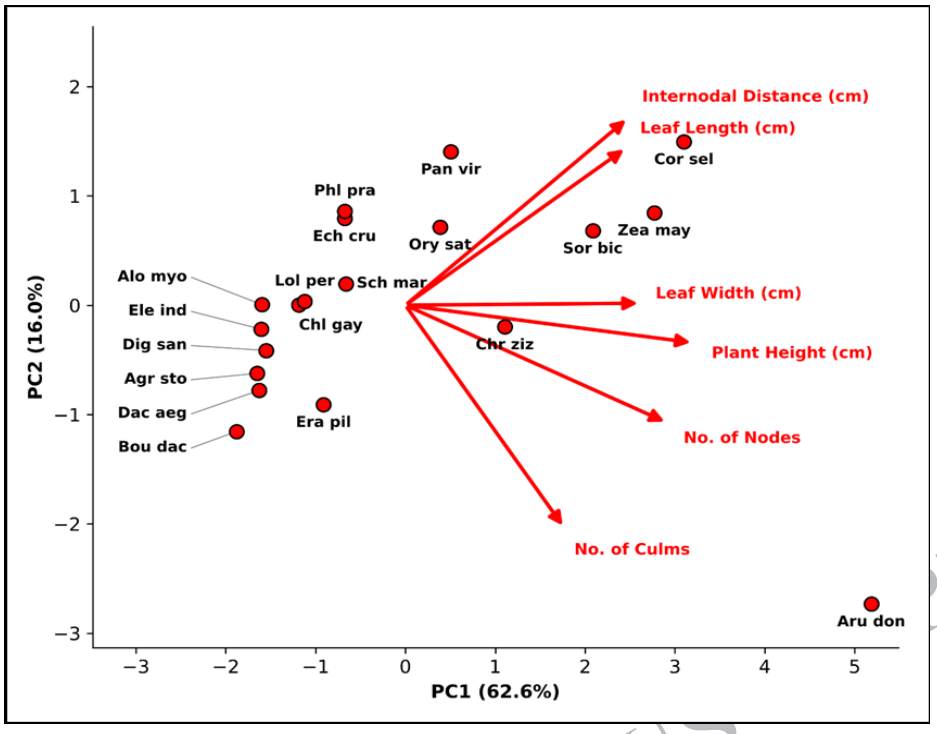


Fig. 1. Principal component analysis (PCA) biplot illustrating functional trait variation among 19 Poaceae species based on six morphological traits. The first two principal components explained 78.6% of total variation (PC1 = 62.6%, PC2 = 16.0%). *Sorghum halepense* and *Thysanolaena maxima* are not shown because their culm, node, and internode data were missing. Red arrows represent trait loadings, with arrow direction indicating trait relationships and length indicating contribution strength. Species codes represent individual taxa (Table 1).

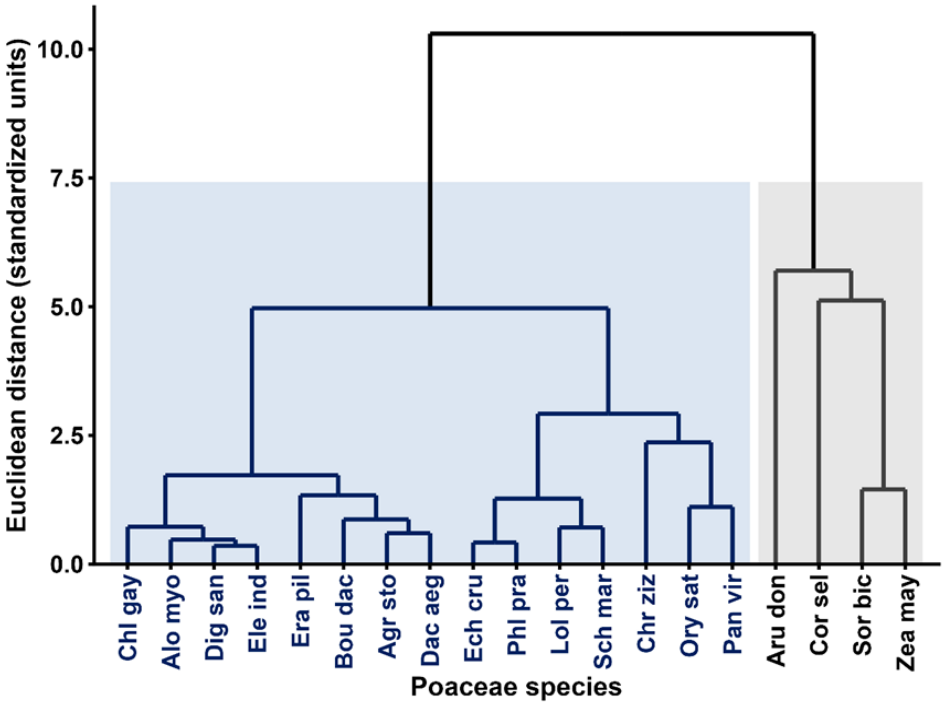


Fig. 2. Hierarchical clustering of functional traits among 19 Poaceae species with complete morphological data. The dendrogram was generated using Euclidean distance and Ward's minimum variance clustering (Ward.D2) based on six standardized morphological traits: plant height, number of culms, number of nodes, internodal distance, leaf length, and leaf width. Colored branches and shading indicate the two clusters identified by silhouette analysis (optimal k = 2; mean silhouette width = 0.54).

3.4. Variation in Stomatal and Epidermal Functional Traits

Micromorphological analysis revealed substantial variation in stomatal characteristics, epidermal structures, and protective traits among the 21 Poaceae species (Table 3). Most species exhibited the typical grass stomatal configuration consisting of dumbbell-shaped guard cells associated with subsidiary cells; however, notable variations were observed in *Sorghum halepense* and *Thysanolaena maxima*, which possessed rectangular and ellipsoid stomatal forms, respectively. Stomatal density varied considerably among species and leaf surfaces. The highest stomatal density was recorded on the abaxial surface of *Oryza sativa* (284 stomata mm^{-2}), followed by *Eragrostis pilosa* (177.5 mm^{-2}) and *Digitaria sanguinalis* (164 mm^{-2}), whereas the lowest abaxial densities occurred in *Arundo donax* (37.5 mm^{-2}) and *Cortaderia selloana* (40.5 mm^{-2}). The stomatal index was highest in *Sorghum halepense* (31.2%) and *Thysanolaena maxima* (25.2%) on the abaxial surface. Trichome-related traits also showed considerable variation. *Sorghum halepense* exhibited the highest trichome index (TI = 7.9%, adaxial), followed by *Eragrostis pilosa* (3.14%, abaxial) and *Thysanolaena maxima* (2.9%, adaxial), whereas trichomes were absent (TI = 0%) in 13 species, including *Agrostis stolonifera*. Variation in epidermal structures was also evident. Species such as *Arundo donax* and *Cortaderia selloana* possessed lignified epidermal cells with silica structures, whereas *Chloris gayana* and *Schizachyrium maritimum* exhibited thick waxy cuticles.

3.5. Multivariate Analysis of Stomatal and Epidermal Traits

PCA based on seven anatomical traits revealed strong separation among Poaceae species and leaf surfaces. The first two principal components explained 90.05% of total variation, with PC1 accounting for 70.21% and PC2 contributing 19.84% (Figure 3; Table 4). PC1 was mainly driven by stomatal architectural traits, including stomatal width (18.73%), stomatal index (18.47%), stomatal density (16.62%), and stomatal length (16.35%). These traits showed high representation quality on PC1 (cos^2 = 0.80–0.92). PC2 was primarily associated with epidermal protection traits, particularly trichome density (37.55%) and trichome index (33.77%). Leaf surfaces showed significant differentiation along both PCA axes. Paired t-tests showed that adaxial and abaxial surfaces differed along PC1 (t_{20} = 9.27, $p < 0.001$) and PC2 (t_{20} = 4.60, $p < 0.001$). PERMANOVA with permutations restricted within species confirmed anatomical separation between leaf surfaces (pseudo-F = 19.55, R^2 = 0.33, p = 0.001), and multivariate dispersion did not differ between surfaces (PERMDISP $F_{1,40}$ = 1.73, p = 0.20). Species including *Dactyloctenium aegyptium, Digitaria sanguinalis*, and *Echinochloa crus-galli* exhibited higher positive scores associated with increased stomatal investment.

The ordination was based on seven standardized anatomical traits after log transformation. The first two principal components explained 90.05% of total variation (PC1 = 70.21%, PC2 = 19.84%). Points represent individual leaf surfaces (adaxial and abaxial), with species labels indicating taxonomic identity. Ellipses represent dispersion of leaf surface groups, and separation between surfaces was tested with paired t-tests and PERMANOVA (see Section 3.5).

3.6. SEM-Based Characterization of Leaf Epidermal Micromorphology

Scanning electron microscopy (SEM) showed differences in leaf-surface micromorphology among the 21 species (Figures 4-10). Each figure shows three species, with the adaxial surface of each species in the upper panel and the abaxial surface in the lower panel. Abaxial stomata were recorded in all species (Table 3). In surface view, they were mostly dumbbell-shaped, but they varied in size, outline and rim thickness, and in the sculpturing of the surrounding cuticle. Several species also had stomata visible on the adaxial surface in SEM (e.g., Figures 5(C), 7(C) and 9(C)), although the light-microscopy counts recorded adaxial stomata in only seven species (Table 3).

Figure 4 shows *Agrostis stolonifera*, *Alopecurus myosuroides* and *Arundo donax*. The adaxial surface of *A. stolonifera* (Figure 4(A)) is finely striated, with long ridges parallel to the leaf axis, and no stomata can be seen at this magnification. Its abaxial surface (Figure 4(B)) has sinuous, irregular cell outlines and a granular cuticle, with small, narrow stomata between the cells; Table 3 records sunken guard cells on this surface. In *A.*

ACCEPTED MANUSCRIPT

Table 3. Stomatal and epidermal trait variation among 21 Poaceae species from Layyah District, Punjab, Pakistan. Traits include stomatal morphology, stomatal size and density, epidermal cell density, trichome density, stomatal index, trichome index, and guard cell characteristics across leaf surfaces. Quantitative values are mean ± SE (n = 3 individuals per species); "–" indicates that stomata were absent.

No.	Plant Specimen	Surface	Stomatal Shape	Stomatal Length µm	Stomatal Width µm	Stomatal Density mm²	Epidermal Cell Density mm²	Trichome Density mm²	SI %	TI %	Guard Cells, Auxiliary Cells
1	*Agrostis stolonifera*	Adaxial	Absent	-	-	-	2150.5 ± 149.5	0 ± 0	0	0	Epidermal cells sinuous
		Abaxial	Dumb-bell	27.5 ± 6.5	5.2 ± 0.7	114.5 ± 4.5	1820.5 ± 99.5	0 ± 0	5.94	0	Guard cells sunken
2	*Alopecurus myosuroides*	Adaxial	Absent	-	-	-	1949.5 ± 24.5	0 ± 0	0	0	Cells rectangular
		Abaxial	Dumb-bell	31.5 ± 4.5	6 ± 0.7	87.5 ± 8.5	1429.5 ± 29.5	0 ± 0	5.80	0	Silica bodies present
3	*Arundo donax*	Adaxial	Absent	-	-	-	1209.5 ± 9.5	0 ± 0	0	0	Epidermal cells silicified
		Abaxial	Dumb-bell	55.5 ± 3.5	10.25 ± 1.25	37.5 ± 8.5	669.5 ± 69.5	0 ± 0	5.37	0	Guard cells with lignified ledges
4	*Bouteloua dactyloides*	Adaxial	Absent	-	-	-	2009.5 ± 9.5	0 ± 0	0	0	Cells isodiametric
		Abaxial	Dumb-bell	26 ± 3	4.95 ± 0.95	141.5 ± 5.5	1569.5 ± 69.5	0 ± 0	8.30	0	Stomata in intercostal zones
5	*Chloris gayana*	Adaxial	Absent	-	-	-	1639.5 ± 39.5	0 ± 0	0	0	Epidermal cells with a thick, waxy cuticle
		Abaxial	Dumb-bell	32.5 ± 4.5	6.25 ± 0.65	124.5 ± 6.5	1149.5 ± 49.5	0 ± 0	9.80	0	Guard cells with cuticular knobs
6	*Chrysopogon zizanioides*	Adaxial	Absent	-	-	-	1379.5 ± 79.5	0 ± 0	0	0	Cells with waxy cuticle
		Abaxial	Dumb-bell	42.5 ± 4.5	7.95 ± 0.15	62.5 ± 3.5	909.5 ± 9.5	0 ± 0	6.47	0	Guard cells with suberized walls
7	*Cortaderia selloana*	Adaxial	Absent	-	-	-	1119.5 ± 19.5	0 ± 0	0	0	Epidermal cells lignified
		Abaxial	Dumb-bell	52.5 ± 5.5	10.2 ± 0.9	40.5 ± 7.5	779.5 ± 79.5	0 ± 0	5.00	0	Guard cells with silica caps
8	*Dactyloctenium aegyptium*	Adaxial	Dumb-bell	25 ± 3	4.9 ± 0.6	17.25 ± 7.25	1669.5 ± 69.5	7.75 ± 0.75	1.06	0.48	Microhairs unicellular
		Abaxial	Dumb-bell	31 ± 4	5.7 ± 0.4	102.5 ± 5.5	1289.5 ± 89.5	24.5 ± 2	7.33	1.94	Guard cells dome-shaped
9	*Digitaria sanguinalis*	Adaxial	Absent	-	-	-	1949.5 ± 49.5	5.75 ± 0.75	0	0.31	Microhairs glandular
		Abaxial	Dumb-bell	31 ± 7	5.75 ± 0.45	164 ± 8	1409.5 ± 9.5	21.75 ± 0.75	10.48	1.56	Guard cells with cuticular horns
10	*Echinochloa crus-galli*	Adaxial	Absent	-	-	-	1779.5 ± 79.5	3.75 ± 0.75	0	0.22	Macrohairs barbed
		Abaxial	Dumb-bell	33 ± 6	6.6 ± 0.5	131.5 ± 9.5	1209.5 ± 9.5	17.25 ± 0.75	9.84	1.40	Guard cells with cuticular ridges

ACCEPTED MANUSCRIPT

11	*Eleusine indica*	Adaxial	Absent	-	-	-	2049.5 ± 49.5	0 ± 0	0	0	Cells with micro-papillae
		Abaxial	Dumb-bell	28 ± 3	5.4 ± 0.5	147.5 ± 6.5	1629.5 ± 29.5	0 ± 0	8.33	0	Stomata in furrows
12	*Eragrostis pilosa*	Adaxial	Dumb-bell	28 ± 4	5.15 ± 1.15	21.5 ± 3.5	1589.5 ± 89.5	11.5 ± 1	1.30	0.69	Microhairs bicellular
		Abaxial	Dumb-bell	29 ± 6	5.6 ± 0.6	177.5 ± 8.5	1209.5 ± 9.5	37.75 ± 0.75	12.82	3.14	Papillate subsidiary cells
13	*Lolium perenne*	Adaxial	Dumb-bell	38.5 ± 6.5	7.45 ± 0.15	41.5 ± 2.5	1319.5 ± 19.5	0 ± 0	3.08	0	Subsidiary cells: 2, parallel
		Abaxial	Dumb-bell	41 ± 2	7.7 ± 0.6	67.5 ± 3.5	1049.5 ± 24.5	0 ± 0	6.09	0	Guard cells thick-walled
14	*Oryza sativa*	Adaxial	Dumb-bell	30.5 ± 4.5	6.4 ± 0.5	34.5 ± 5.5	1119.5 ± 19.5	0 ± 0	3.03	0	Subsidiary cells inflated
		Abaxial	Dumb-bell	33.5 ± 4.5	6.85 ± 0.55	284 ± 14.5	889.5 ± 89.5	0 ± 0	24.26	0	Papillae around stomata
15	*Panicum virgatum*	Adaxial	Absent	-	-	-	1539.5 ± 39.5	0 ± 0	0	0	Cells polygonal
		Abaxial	Dumb-bell	35.5 ± 3.5	7.2 ± 0.7	78.5 ± 6.5	1049.5 ± 49.5	0 ± 0	6.91	0	
16	*Phleum pratense*	Adaxial	Absent	-	-	-	1859.5 ± 59.5	0 ± 0	0	0	Cells elongated
		Abaxial	Dumb-bell	35 ± 8	6.65 ± 0.55	91.5 ± 5.5	1339.5 ± 39.5	0 ± 0	6.43	0	Subsidiary cells overarching
17	*Schizachyrium maritimum*	Adaxial	Absent	-	-	-	1719.5 ± 19.5	0 ± 0	0	0	Epidermal cells with a thick waxy cuticle
		Abaxial	Dumb-bell	30 ± 5	5.75 ± 0.75	117.5 ± 8.5	1249.5 ± 49.5	0 ± 0	8.63	0	
18	*Sorghum bicolor*	Adaxial	Absent	-	-	-	1429.5 ± 29.5	3.75 ± 0.75	0	0.28	Macrohairs near veins
		Abaxial	Dumb-bell	42 ± 3	8.2 ± 0.7	86.5 ± 6.5	949.5 ± 49.5	14.75 ± 0.75	8.39	1.58	Subsidiary cells crescent-shaped
19	*Sorghum halepense*	Adaxial	Rectangular	31 ± 6	18 ± 1	62.5 ± 5.5	289.5 ± 89.5	24.75 ± 0.75	17.6	7.9	Dumbbell-shaped; subsidiary cells indistinct
		Abaxial	Rectangular	35.5 ± 3.5	20.25 ± 0.95	144.5 ± 6.5	319.5 ± 19.5	17.75 ± 0.75	31.2	5.3	Dumbbell-shaped; subsidiary cells indistinct
20	*Thysanolaena maxima*	Adaxial	Ellipsoid	37.5 ± 5.5	22.15 ± 1.85	84.5 ± 5.5	409.5 ± 9.5	11.75 ± 0.75	17.2	2.9	Dumbbell-shaped; 2 subsidiary cells
		Abaxial	Ellipsoid	42 ± 4	24.25 ± 1.25	127 ± 7	379.5 ± 79.5	7.75 ± 0.75	25.2	2.1	Dumbbell-shaped; 2 subsidiary cells
21	*Zea mays L.*	Adaxial	Dumb-bell	45 ± 4	8.95 ± 0.85	27.5 ± 6.5	979.5 ± 30.5	2.99 ± 0.09	2.78	0.31	Subsidiary cells triangular
		Abaxial	Dumb-bell	47.5 ± 5.5	9.35 ± 0.45	95.25 ± 4.25	760.5 ± 13.5	11.75 ± 0.75	11.11	1.58	Macrohairs near the midrib

ACCEPTED MANUSCRIPT

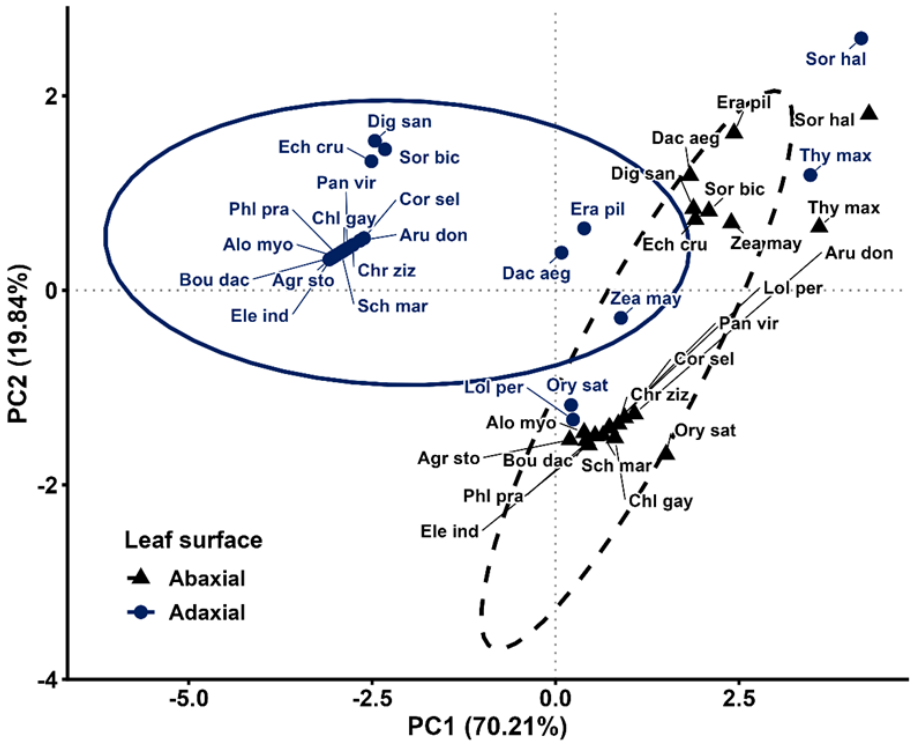


Fig. 3. Principal component analysis showing variation in stomatal and epidermal functional traits among Poaceae species.

myosuroides, the adaxial view (Figure 4(C)) shows an elliptic stomatal complex with a raised, smooth rim and a narrow, slit-like pore in a folded cuticle. The abaxial view (Figure 4(D)) shows a stoma with a lens-shaped aperture bordered by thick guard-cell walls. *Arundo donax* looks different from the other two. Its adaxial surface (Figure 4(E)) is coarse and densely wrinkled, with scattered surface deposits, which fits the silicified epidermal cells noted in Table 3. Its abaxial stoma (Figure 4(F)) is large, with a long pore and thickened ledges, and this species had the longest stomata in the data set (55.5 µm; Table 3).

Figure 5 shows *Bouteloua dactyloides*, *Chloris gayana,* and *Chrysopogon zizanioides*. The adaxial surface of *B. dactyloides* (Figure 5(A)) is made up of elongated, ridged cells, with an elongated, tapering outgrowth lying along the surface. On the abaxial surface (Figure 5(B)), a stoma with a narrow, slit-like pore and a finely toothed rim sits between cell ridges in the intercostal zone, as recorded in Table 3. In *C. gayana*, stomata with prominent, thick rims are sunk among strongly folded cuticular ridges, so the surface looks deeply sculptured (Figure 5(C)). At low magnification (Figure 5(D)), the surface is covered with a dense, uniform network of wrinkled cuticular folds, which matches the thick, waxy cuticle recorded for this species (Table 3). In *C. zizanioides*, Figure 5(E), shows a stoma whose narrow pore is partly covered by an irregular cuticular layer and surface deposit.

ACCEPTED MANUSCRIPT

Table 4. PCA eigenvalues, explained variance, and cumulative variance of stomatal and epidermal traits among Poaceae species.

Principal component	Eigenvalue	Variance explained (%)	Cumulative variance (%)
PC1	4.91	70.21	70.21
PC2	1.39	19.84	90.05
PC3	0.53	7.50	97.55
PC4	0.13	1.83	99.39
PC5	0.03	0.47	99.86

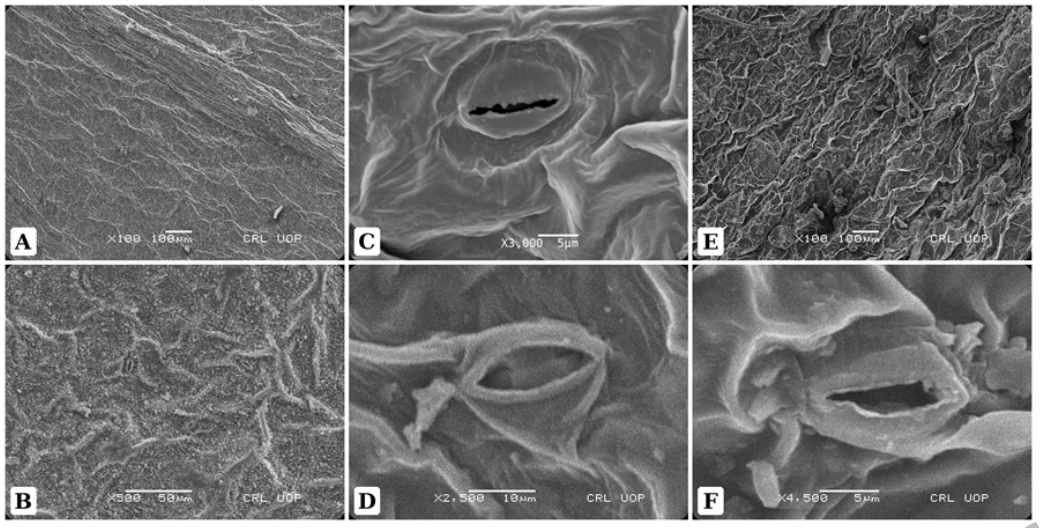


Fig. 4. SEM micrographs of the leaf epidermis. (A) Adaxial and (B) abaxial leaf surface of *Agrostis stolonifera*; (C) adaxial and (D) abaxial leaf surface of *Alopecurus myosuroides*; (E) adaxial and (F) abaxial leaf surface of *Arundo donax*. Magnification and scale bars are shown on each micrograph.

Figure 5(F) shows a strongly striated surface with longitudinal ridges and elongated cells along the veins, which fits its waxy cuticle (Table 3).

Figure 6 shows *Cortaderia selloana*, *Dactyloctenium aegyptium* and *Digitaria sanguinalis*. The adaxial surface of *C. selloana* (Figure 6(A)) is covered with an irregular network of raised cuticular ridges and wax particles. Its abaxial stoma (Figure 6(B)) has a thick, raised rim and a slit-like pore, and the stomata of this species were among the largest measured (52.5 µm; Table 3). *Dactyloctenium aegyptium* has a heavily folded, ridged adaxial surface with surface deposits (Figure 6(C)). Its abaxial stoma (Figure 6(D)) has prominent, dome-shaped guard cells around a lens-shaped pore, as recorded in Table 3. In *D. sanguinalis*, Figure 6(E) shows a stoma with a smooth, raised guard-cell rim. Figure 6(F) shows a long, tapering macrohair that rises from a swollen base on a finely reticulate surface, which agrees with the high abaxial trichome density of this species (21.75 mm^{-2}; Table 3).

ACCEPTED MANUSCRIPT

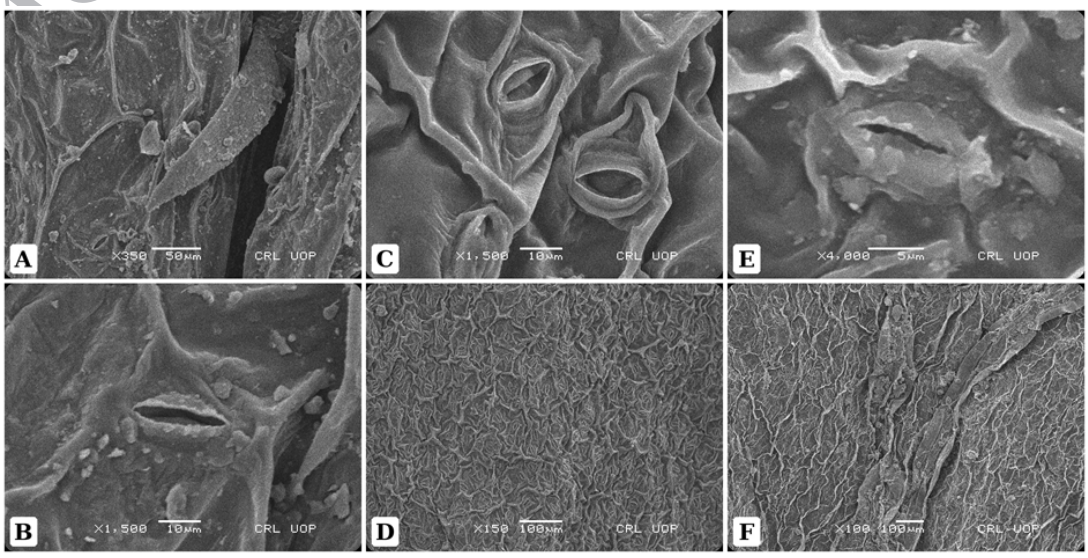


Fig. 5. SEM micrographs of the leaf epidermis. (A) Adaxial and (B) abaxial leaf surface of *Bouteloua dactyloides*; (C) adaxial and (D) abaxial leaf surface of *Chloris gayana*; (E) adaxial and (F) abaxial leaf surface of *Chrysopogon zizanioides*. Magnification and scale bars are shown on each micrograph.

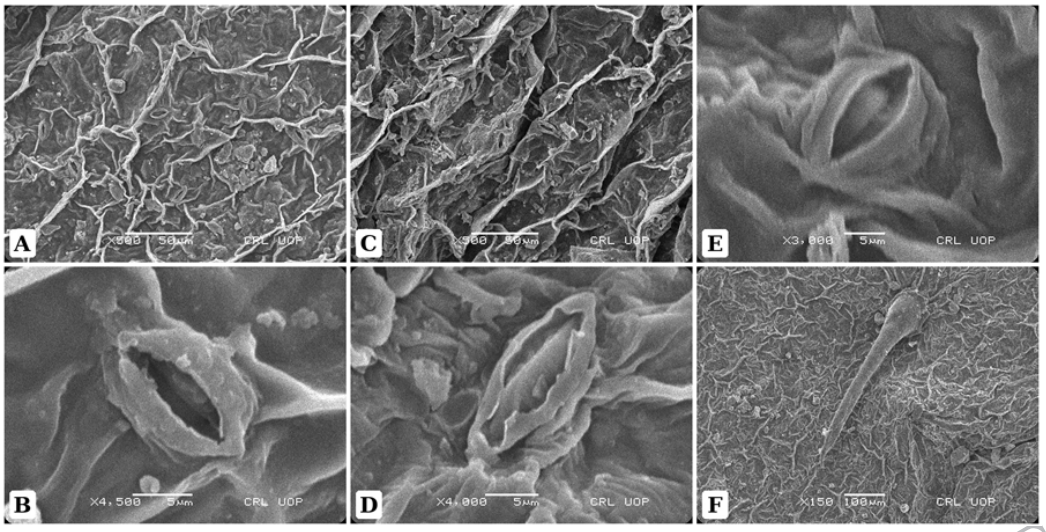


Fig. 6. SEM micrographs of the leaf epidermis. (A) Adaxial and (B) abaxial leaf surface of *Cortaderia selloana*; (C) adaxial and (D) abaxial leaf surface of *Dactyloctenium aegyptium*; (E) adaxial and (F) abaxial leaf surface of *Digitaria sanguinalis*. Magnification and scale bars are shown on each micrograph.

Figure 7 shows *Echinochloa crus-galli*, *Eleusine indica* and *Eragrostis pilosa*. In *E. crus-galli*, the stomatal complex has a thick, smooth rim and an elliptic pore surrounded by cuticular ridges (Figure 7(A)). On a reticulate surface, several long, stiff macrohairs rise together from a swollen basal cushion (Figure 7(B)), which fits the barbed macrohairs recorded for this species (Table 3). *Eleusine indica* has many small stomata arranged in longitudinal rows between wavy cell walls (Figure 7(C)). At low magnification, its surface is finely wrinkled, with a single prickle-like outgrowth near a vein (Figure 7(D)). *Eragrostis pilosa* has elongated, parallel long cells with spindle-shaped hairs lying along the leaf axis (Figure 7(E)). On its abaxial surface (Figure 7(F)), small stomata are arranged in rows between the long cells, and rows of papillae run along some cell files. This agrees with the papillate subsidiary cells and the high abaxial stomatal density (177.5 mm^{-2}) recorded in Table 3.

Figure 8 shows *Lolium perenne*, *Oryza sativa* and *Panicum virgatum*. In *L. perenne*, two stomata

ACCEPTED MANUSCRIPT

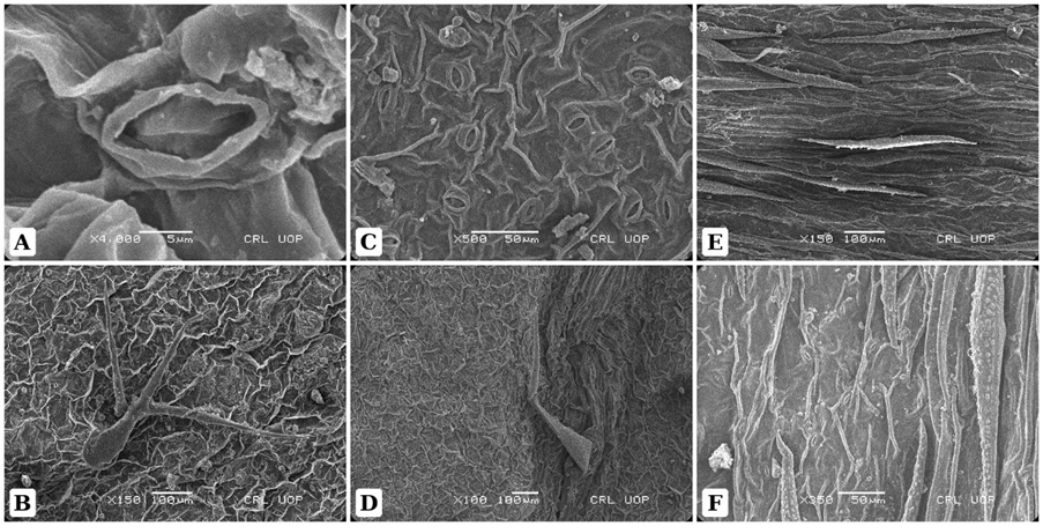


Fig. 7. SEM micrographs of the leaf epidermis. (A) Adaxial and (B) abaxial leaf surface of *Echinochloa crus-galli*; (C) adaxial and (D) abaxial leaf surface of *Eleusine indica*; (E) adaxial and (F) abaxial leaf surface of *Eragrostis pilosa*. Magnification and scale bars are shown on each micrograph.

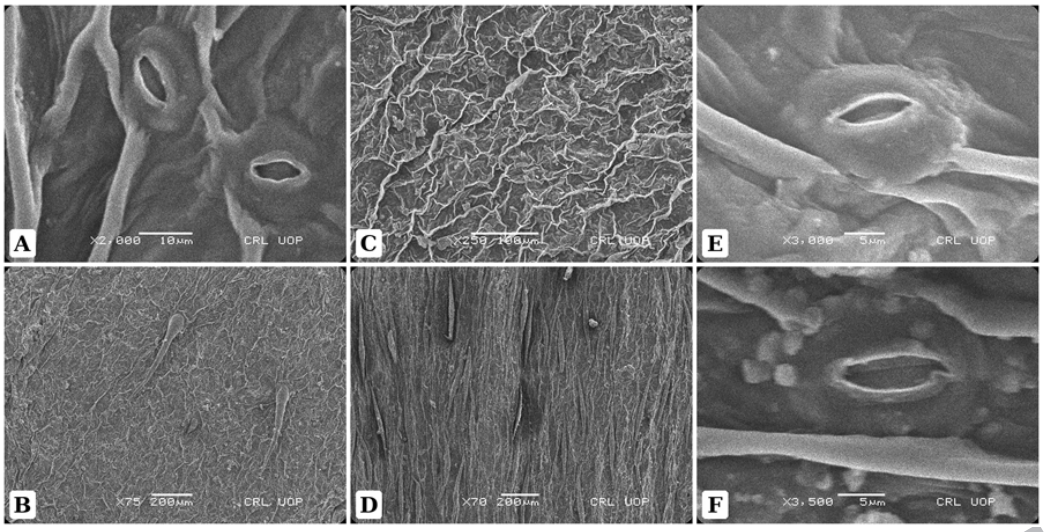


Fig. 8. SEM micrographs of the leaf epidermis. (A) Adaxial and (B) abaxial leaf surface of *Lolium perenne*; (C) adaxial and (D) abaxial leaf surface of *Oryza sativa*; (E) adaxial and (F) abaxial leaf surface of *Panicum virgatum*. Magnification and scale bars are shown on each micrograph.

with thick, raised rims and elliptic pores lie between smooth, elongated cell ridges (Figure 8(A)). At low magnification (Figure 8(B)), the surface is evenly wrinkled and has scattered, short hair-like outgrowths with swollen bases. *Oryza sativa* has a strongly reticulate surface with irregular cuticular ridges (Figure 8(C)). Its abaxial surface (Figure 8(D)) is made up of long, narrow cells in parallel files, with scattered, spindle-shaped prickles along the veins. In *Panicum virgatum*, both surfaces have smooth, elliptic stomatal complexes with narrow, lens-shaped pores, bordered by smooth long-cell walls (Figure 8(E & F)). The abaxial surface also has small surface granules (Figure 8(F)).

Figure 9 shows *Phleum pratense*, *Schizachyrium maritimum* and *Sorghum bicolor*. In *P. pratense*, several stomata with distinct guard-cell rims are scattered among irregular, ridged cells with surface debris (Figure 9(A)). A single abaxial stoma has guard cells partly overarched by the surrounding subsidiary cells (Figure 9(B)), which is the feature Table 3 records for this species. *Schizachyrium maritimum* has many stomata with elliptic outlines set among strongly folded cuticular ridges (Figure 9(C)). At higher magnification, one stoma has thick, rounded guard cells and a straight pore (Figure 9(D)). *Sorghum bicolor* has a smooth adaxial surface with fine, branching ridges (Figure

ACCEPTED MANUSCRIPT

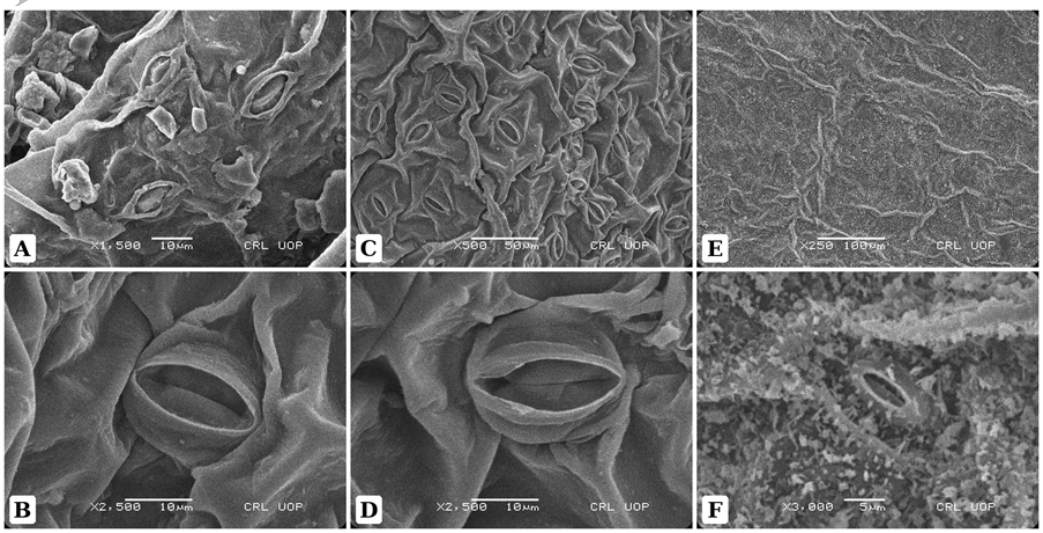


Fig. 9. SEM micrographs of the leaf epidermis. (A) Adaxial and (B) abaxial leaf surface of *Phleum pratense*; (C) adaxial and (D) abaxial leaf surface of *Schizachyrium maritimum*; (E) adaxial and (F) abaxial leaf surface of *Sorghum bicolor*. Magnification and scale bars are shown on each micrograph.

9(E)). On its abaxial surface (Figure 9(F)), a small stoma with a narrow pore is surrounded by dense, granular wax deposits.

Figure 10 shows *Sorghum halepense*, *Thysanolaena maxima* and *Zea mays*. The adaxial surface of *S. halepense* (Figure 10(A)) has several stomatal complexes among irregular cuticular ridges and fine wax flakes. Each has a rectangular to oval outline and raised rims around a narrow, irregular pore. Its abaxial stoma (Figure 10(B)) has thickened guard cells around a straight pore, and the subsidiary cells cannot be clearly told apart in surface view (Table 3). *Thysanolaena maxima* have an elliptic stomatal outline on both surfaces (Figure 10(C & D)), with a smooth, thick rim and a wide, lens-shaped pore. This matches the ellipsoid stomata and the large stomatal width (22.15-24.25 µm) recorded in Table 3. At low magnification, *Zea mays* have small stomata scattered between long cells on both surfaces (Figure 10(E & F)). A large, pointed macrohair is visible on the adaxial surface (Figure 10(E)), in agreement with the macrohairs recorded for this species (Table 3).

3.7. Overview of Trait Differentiation

Poaceae occupies environments ranging from humid ecosystems to highly water-limited arid landscapes [4, 41]. The 21 species studied here from Layyah District differed markedly in plant architecture and leaf-epidermal traits. The first two morphological PCA axes (19 species) explained 78.6% of trait variation and were dominated by plant size and leaf dimensions, whereas the first two anatomical PCA axes explained 90.05% of variation and were dominated by stomatal size, density, and index. Because neither environmental variables (e.g., soil moisture, texture, or salinity) nor physiological performance (e.g., stomatal conductance, water-use efficiency, or drought survival) was measured, the functional interpretations below are hypotheses based on published trait–function relationships rather than tested adaptations. Differences among species may also partly reflect species identity and phylogenetic history rather than local habitat conditions.

3.8. Functional Differentiation of Poaceae Species through Morphological Trait Variation

Considerable variation in plant architecture among the studied species may reflect contrasting strategies of resource acquisition and conservation. The morphological PCA identified plant height, leaf dimensions, internodal distance, and vegetative structure as the dominant traits separating species. Large-bodied grasses, including *Arundo donax*, *Cortaderia selloana*, *Sorghum bicolor*, and *Zea mays*, were strongly associated with positive PC1 scores, reflecting their larger size and greater structural development. In contrast, smaller species such as *Bouteloua dactyloides, Agrostis stolonifera, Dactyloctenium aegyptium*, and *Digitaria sanguinalis* occupied the negative region

ACCEPTED MANUSCRIPT

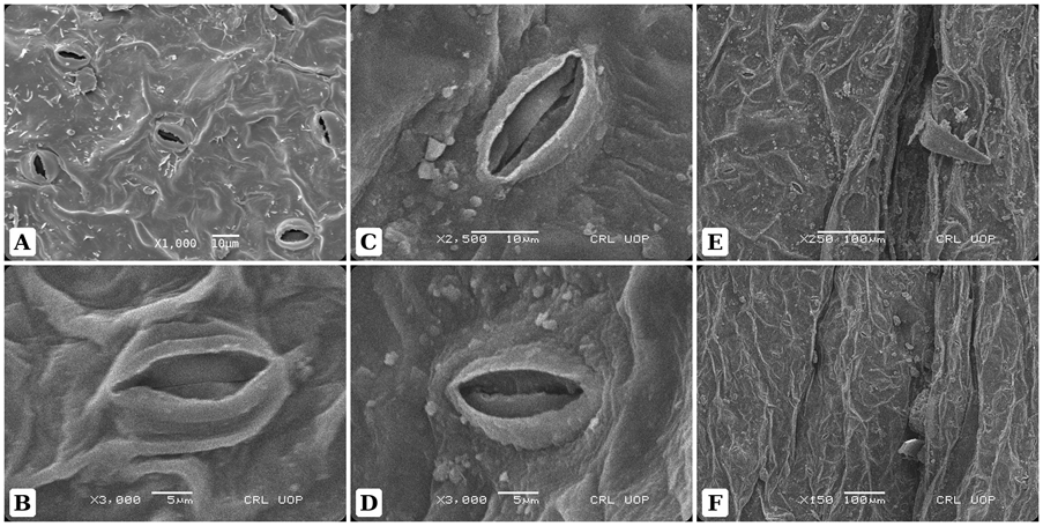


Fig. 10. SEM micrographs of the leaf epidermis. (A) Adaxial and (B) abaxial leaf surface of *Sorghum halepense*; (C) adaxial and (D) abaxial leaf surface of *Thysanolaena maxima*; (E) adaxial and (F) abaxial leaf surface of *Zea mays*. Magnification and scale bars are shown on each micrograph.

of PC1, reflecting compact growth forms. Large plant size and extended internodes are commonly associated with habitats where water and nutrients are relatively abundant, as increased leaf area and vertical growth enhance light capture and competitive ability. The exceptional height and internodal elongation of *Arundo donax* indicate a strategy based on rapid biomass accumulation and efficient resource exploitation, consistent with observations that tall perennial grasses generally dominate moist or nutrient-rich habitats [42, 43]. Conversely, published work suggests that reduced stature and shorter internodes in drought-adapted grasses may represent a conservative strategy that minimizes water demand and maintains physiological stability under stressful conditions [44]. Smaller leaves reduce transpirational surface area, whereas compact architecture decreases hydraulic limitations during periods of moisture scarcity.

Hierarchical clustering supported the main PCA axis, separating four large grasses (*Arundo donax*, *Cortaderia selloana*, *Sorghum bicolor*, and *Zea mays*) from 15 smaller species, with a reasonable clustering structure (mean silhouette width = 0.54). This grouping is consistent with the range of grass strategies, from rapid resource acquisition to stress tolerance, reported in other studies [45, 46], although testing whether these groups differ in habitat or performance would require environmental and physiological data.

3.9. Stomatal and Epidermal Differentiation among Species and Leaf Surfaces

Leaf anatomical traits represent critical mechanisms through which plants regulate carbon gain and water loss, particularly under arid and semi-arid conditions [47, 48]. The present study revealed substantial interspecific variation in stomatal architecture, density, and epidermal characteristics. Anatomical PCA demonstrated that stomatal width, stomatal index, stomatal density, and stomatal length were the primary contributors to PC1, collectively explaining the majority of anatomical variation among species. Because stomatal size and density set the maximum capacity for gas exchange, these traits probably matter for gas exchange, although their link to drought tolerance in these species remains to be tested.

Adaxial and abaxial surfaces differed consistently (Section 3.5), mainly because stomata were absent from, or sparse on, the adaxial surface of most species (Table 3). Most species exhibited typical grass-type dumbbell-shaped stomata, a characteristic feature associated with rapid stomatal movement and efficient regulation of transpiration. However, deviations from this pattern, including rectangular stomata in *Sorghum halepense* and ellipsoid stomata in *Thysanolaena maxima*, may reflect species-specific modifications of the stomatal complex. Studies of plants from water-limited habitats have linked such anatomical features to improved water conservation [49, 50]. A higher stomatal index and specialized stomatal arrangements observed in species such as *Sorghum halepense* and *Thysanolaena maxima* may enhance regulation of gas exchange under fluctuating temperature and moisture conditions. Previous studies have demonstrated that stomatal size, density, and distribution strongly influence drought tolerance by balancing photosynthetic activity with transpirational water loss [51, 52]. Conversely, *Agrostis stolonifera*, a species typical of moister temperate habitats, had a low stomatal index; whether this reflects weaker selection for water conservation cannot be determined from the present data [25, 53].

3.10. Trichomes, Epidermal Structures, and Protective Traits

Variation in trichome density and epidermal characteristics points to additional protective traits in the studied species [54]. Trichomes contribute to drought tolerance by reducing boundary layer disruption, limiting excessive radiation exposure, and providing protection against herbivory [55]. In the present study, *Eragrostis pilosa*, *Sorghum halepense*, and *Dactyloctenium aegyptium* had the highest trichome densities (Table 3), which may provide protection in dry and exposed habitats. Similar protective roles of trichomes have been documented in grasses growing under high-temperature and water-limited conditions [56, 57].

SEM observations further revealed considerable diversity in epidermal architecture, including silica bodies, papillae, cuticular ridges, and specialized surface structures. Species such as *Arundo donax* and *Cortaderia selloana* showed silicified or lignified epidermal cells and protective

ACCEPTED MANUSCRIPT

surface modifications, which may reduce water loss and increase mechanical resistance. Silica deposition and cuticular reinforcement represent important evolutionary strategies in grasses, providing both mechanical protection and improved water conservation [17, 58].

Waxy surfaces and thick cuticles in several species are consistent with tolerance of high evaporative demand, although cuticular permeability was not measured. Such modifications reduce uncontrolled water diffusion through epidermal surfaces while maintaining photosynthetic efficiency. Similar relationships between epidermal specialization, drought resistance, and herbivore defence have been reported across xeric grass ecosystems [59, 60].

3.11. Xeromorphic Epidermal Traits and C_4 Photosynthesis in Poaceae

Several species showed epidermal characteristics usually described as xeromorphic. Lignified and silicified epidermal cells and specialized guard cell structures (lignified ledges and silica caps) observed in *Arundo donax* and *Cortaderia selloana*, together with apparently sunken guard cells in *Agrostis stolonifera* (Table 3), are features commonly associated with reduced transpiration. Because SEM records only the leaf surface, the depth of stomatal sinking should be confirmed with transverse sections. Such traits could be advantageous in Layyah, where high summer temperatures and irregular rainfall are expected to favour water conservation, but this hypothesis requires physiological testing.

Several of the studied species, including *Panicum virgatum*, *Schizachyrium maritimum*, *Sorghum bicolor*, and *Zea mays*, are known C_4 grasses [5, 28]. Kranz anatomy, however, is an internal leaf feature that cannot be assessed from epidermal SEM images, so it was not evaluated in this study; transverse leaf sections would be needed to link the epidermal traits reported here with Kranz-type organization. C_4 metabolism provides a physiological advantage by maintaining high photosynthetic efficiency while reducing water loss, making these species particularly successful in warm semi-arid environments [61, 62]. Guard cell and subsidiary cell morphology also differed among species. In *Sorghum bicolor*, specialized subsidiary cell structures may facilitate rapid stomatal responses, improving regulation of water loss during heat stress. Similar relationships between stomatal architecture and hydraulic efficiency have been reported in drought-resistant grasses [25, 63].

3.12. Potential Ecological and Agricultural Relevance

Differences in plant architecture and leaf-epidermal traits suggest that the species could occupy different niches. Structural diversity within grass communities has been linked elsewhere to soil protection, nutrient cycling, and resilience to climatic fluctuations [64, 65]. These functions were not measured here, so the links remain untested for Layyah. Several studied species also have direct agricultural importance. *Zea mays*, *Sorghum bicolor*, and *Oryza sativa* represent globally important crops whose anatomical traits influence productivity under changing climates. Published studies show that stomatal control of water loss contributes to their performance under drought [66, 67]; the epidermal data presented here provide a baseline for comparing these crops with co-occurring wild grasses. Additionally, extensive root systems of grasses improve soil stability, reduce erosion, and enhance water retention, making Poaceae essential components of sustainable agroecosystems in semi-arid regions [7, 68].

This study has several limitations that should be considered when interpreting the results. First, morphological and foliar traits were measured in only three individuals per species. Although this sampling provides an initial basis for interspecific comparison, the limited replication may not fully capture within-species variation; therefore, species-level trait estimates should be interpreted cautiously. Second, each species was sampled once, during its flowering period, precluding an assessment of seasonal variation in leaf traits, including stomatal density. Third, scanning electron microscopy (SEM) provided information on leaf-surface characteristics but did not reveal internal anatomical features, such as Kranz anatomy or the degree of stomatal sinking, which require transverse leaf sections. Fourth, environmental variables and physiological attributes were not measured, limiting our ability to establish relationships between observed trait differences, habitat conditions, and plant performance.

ACCEPTED MANUSCRIPT

In addition, specimen-level habitat information was not recorded systematically, preventing rigorous comparisons of traits among the four habitat types represented in the study. Future studies should address these limitations through larger within-species sample sizes, repeated seasonal sampling, systematic recording of habitat conditions, and anatomical analyses of transverse leaf sections. Integrating environmental measurements with physiological assessments, including stomatal conductance and water-use efficiency, would further help evaluate the ecological significance of the observed trait variation and test potential trait–environment relationships. Despite these limitations, the 21 Poaceae species examined from Layyah District exhibited interspecific variation primarily in plant-size-related, stomatal, and trichome traits, alongside consistent differences between the adaxial and abaxial leaf surfaces. These findings provide a comparative morphological and foliar-anatomical baseline for further taxonomic investigation and generate hypotheses regarding the potential relationships between grass functional traits, habitat conditions, and drought adaptation. However, these ecological interpretations require further testing using directly measured environmental and physiological data.

4. CONCLUSIONS

The 21 Poaceae species from Layyah District exhibited substantial variation in plant architecture and leaf epidermal characteristics. In the 19 species with complete data, plant height, node number, leaf dimensions, and internodal distance separated four large grasses from 15 smaller species. Stomatal size, density, and index were the principal epidermal traits differentiating species, with consistent differences between adaxial and abaxial leaf surfaces. Scanning electron microscopy further revealed variation in trichomes, silica bodies, papillae, and cuticular features, providing valuable taxonomic evidence for interspecific comparisons. Although some of these characteristics are associated with water conservation, their adaptive significance remains untested because environmental conditions and physiological performance were not measured. This study establishes a comparative baseline for the morphological and foliar characterization of Poaceae in Layyah District. Future research integrating larger sample sizes, habitat assessments, transverse leaf anatomy, and physiological measurements will help clarify trait-environment relationships and evaluate potential contributions to drought tolerance.

5. ACKNOWLEDGEMENTS

The authors are grateful to the Department of Botany, PMAS Arid Agriculture University, Rawalpindi, for providing laboratory facilities. We thank the local communities of Layyah District for their cooperation during field sampling.

6. ETHICAL STATEMENT

This study was conducted in compliance with institutional guidelines for plant collection and research. During this study no human participants, human subjects, or animals were involved; therefore, ethical approval was not required.

7. AUTHORSHIP CONTRIBUTIONS

Rafia Nawaz: Investigation, Data curation, Writing – original draft. Khafsa Malik: Conceptualization, Methodology, Supervision, Writing – review & editing. Muhammad Imran: Formal analysis, Visualization, Writing – review & editing. Ubaidur Rahman: Investigation, Resources. Najeeb Ullah: Formal analysis, Validation. Bushra Ali: Investigation, Writing – review & editing. All authors read and approved the final manuscript.

8. FUNDING

No funding was received for this research.

9. CONFLICT OF INTEREST

The authors declare that they have no known competing commercial interests or personal relationships that could have appeared to influence the work reported in this paper.

10. DECLARATION

The authors declare that the results presented in this manuscript are original and that the same material has neither been published previously nor is currently under consideration for publication elsewhere. AI tools, including ChatGPT, were used only for English-language refinement, readability, and editorial improvement. All scientific content, results, analyses, and conclusions were

ACCEPTED MANUSCRIPT

independently reviewed and verified by the authors, who remain fully responsible for the manuscript. All authors have approved the final version of the manuscript and agree to its submission for publication. In case the article is accepted for publication, its copyright will be assigned to the Pakistan Academy of Sciences.

11. REFERENCES

1. Z. Xu and Z. Guoning Gramineae (Eds.). Identification and Control of Common Weeds. Volume 1. *Zhejiang University Press, Springer* (2017). DOI:10.1007/978-94-024-0954-3
2. C. Bell. Native grasslands. In: Grasses: Crops, Competitors, and Ornamentals. H. Kraehmer (Ed.). *John Wiley* & Sons, *Hoboken, NJ, USA* pp. 517-548 (2019). https://doi.org/10.1002/9781119417095.ch17
3. M.N. Khan, S. Ali, T. Yaseen, S. Ullah, A. Zaman, M. Iqbal, and S. Shah. Eco-taxonomic study of family Poaceae (Gramineae). *RADS Journal of Biological Research & Applied Sciences* 10(2): 63-75 (2020). https://doi.org/10.37962/jbas.v10i2.191
4. T.R. Hodkinson. Evolution and taxonomy of the grasses (Poaceae): a model family for the study of species-rich groups. *Annual Plant Reviews Online* 1: 255-294 (2018). https://doi.org/10.1002/9781119312994.apr0622
5. W. Huang, L. Zhang, J.T. Columbus, Y. Hu, Y. Zhao, L. Tang, Z. Guo, W. Chen, M. McKain, M. Bartlett, C.-H. Huang, D.-Z. Li, S. Ge, and H. Ma. A well-supported nuclear phylogeny of Poaceae and implications for the evolution of C4 photosynthesis. *Molecular Plant* 15(4): 755-777 (2022). https://doi.org/10.1016/j.molp.2022.01.015
6. M.R. Lundgren, C.P. Osborne, and P.-A. Christin. Deconstructing Kranz anatomy to understand C4 evolution. *Journal of Experimental Botany* 65(13): 3357-3369 (2014). https://doi.org/10.1093/jxb/eru186
7. F. Ojija. Perennial grasses: natural allies for soil health and biodiversity, climate change mitigation, and invasive plant management. *Grass Research* 4(1): e020 (2024). https://doi.org/10.48130/grares-0024-0019
8. K. Klumpp and D.A. Fornara. The carbon sequestration of grassland soils—climate change and mitigation strategies. In: *Sustainable* Meat *and* Milk Production *from* Grasslands. B. Horan, D. Hennessy, M. O'Donovan, E. Kennedy, B. McCarthy, J.A. Finn, and B. O'Brien (Eds.). *Proceedings of the 27th General Meeting of the European Grassland Federation, 17th - 21st June 2018, Cork, Ireland. Grassland Science in Europe* 23: 509 (2018). https://www.europeangrassland.org/fileadmin/documents/Infos/Printed_Matter/Proceedings/EGF2018.pdf
9. J. Bengtsson, J.M. Bullock, B. Egoh, C. Everson, T. Everson, T. O'Connor, P.J. O'Farrell, H.G. Smith, and R. Lindborg. Grasslands—more important for ecosystem services than you might think. *Ecosphere* 10(2): e02582 (2019). https://doi.org/10.1002/ecs2.2582
10. C.A.E. Strömberg. Evolution of grasses and grassland ecosystems. *Annual Review of Earth and Planetary Sciences* 39: 517-544 (2011). https://doi.org/10.1146/annurev-earth-040809-152402
11. C.C. Daehler. Performance comparisons of co-occurring native and alien invasive plants: implications for conservation and restoration. *Annual Review of Ecology, Evolution, and Systematics* 34: 183-211 (2003). https://doi.org/10.1146/annurev.ecolsys.34.011802.132403
12. M. Shavanov. The role of food crops within the Poaceae and Fabaceae families as nutritional plants. *IOP Conference Series: Earth and Environmental Science* 624(1): 012111 (2021). https://doi.org/10.1088/1755-1315/624/1/012111
13. S. Chand, Indu, R.K. Singhal, and P. Govindasamy. Agronomical and breeding approaches to improve the nutritional status of forage crops for better livestock productivity. *Grass and Forage Science* 77(1): 11-32 (2022). https://doi.org/10.1111/gfs.12557
14. Z. Ortega, I. Bolaji, L. Suárez, and E. Cunningham. A review of the use of giant reed (*Arundo donax* L.) in the biorefineries context. *Reviews in Chemical Engineering* 40(3): 305-328 (2024). https://doi.org/10.1515/revce-2022-0069
15. M. Rzanny, H.C. Wittich, P. Mäder, A. Deggelmann, D. Boho, and J. Wäldchen. Image-based automated recognition of 31 Poaceae species: The most relevant perspectives. *Frontiers in Plant Science* 12: 804140 (2022). https://doi.org/10.3389/fpls.2021.804140
16. T.D. Leandro, V.L. Scatena, and L.G. Clark. Comparative leaf blade anatomy and micromorphology in the systematics and phylogeny of Bambusoideae (Poaceae: Poales). *Botanical Journal of the Linnean Society* 192(1): 165-183 (2020). https://doi.org/10.1093/botlinnean/boz074
17. A.S. Khan, M.A. Butt, S.N. Shah, M. Ahmad, S. Kayani, and M. Birjees. Leaf epidermal morphology and its systematic implications in Poaceae: investigating 15 taxa from wetland areas. *Pakistan Journal of Botany* 54(6): 2281-2289 (2022). https://

ACCEPTED MANUSCRIPT

doi.org/10.30848/PJB2022-6(26)

18. M. Keshavarzi. An overview of ecological anatomy of Poaceae halophytes from Iran. In: Handbook of Halophytes: From Molecules to Ecosystems towards Biosaline Agriculture. M.-N. Grigore (Ed.). *Springer, Cham, Switzerland* pp. 1035-1062 (2021). https://doi.org/10.1007/978-3-030-57635-6_35
19. D.M. Blumenthal, K.E. Mueller, J.A. Kray, T.W. Ocheltree, D.J. Augustine, and K.R. Wilcox. Traits link drought resistance with herbivore defence and plant economics in semi-arid grasslands: The central roles of phenology and leaf dry matter content. *Journal of Ecology* 108(6): 2336-2351 (2020). https://doi.org/10.1111/1365-2745.13454
20. N. Harun, S. Shaheen, M. Ahmad, and M.N. Shahid. Light and scanning electron microscopy-based foliar micro morphological tools for the identification of fodder grass taxa. *Microscopy Research and Technique* 83(8): 953-978 (2020). https://doi.org/10.1002/jemt.23490
21. A. Usma, M. Ahmad, M. Zafar, M.I. Ali, O. Kilic, F.A. Ozdemir, S. Sultana, A. Nazir, F. Anjum, and N. Kalsoom. Taxonomic significance of caryopsis in subfamily Panicoideae (Poaceae) using scanning electron microscopy and light microscopy. *Microscopy Research and Technique* 82(10): 1649-1659 (2019). https://doi.org/10.1002/jemt.23331
22. M.M. Waqas, S.H.H. Shah, U.K. Awan, M. Waseem, I. Ahmad, M. Fahad, Y. Niaz, and S. Ali. Evaluating the impact of climate change on water productivity of maize in the semi-arid environment of Punjab, Pakistan. *Sustainability* 12(9): 3905 (2020). https://doi.org/10.3390/su12093905
23. S. Bachle and J.B. Nippert. Microanatomical traits track climate gradients for a dominant C4 grass species across the Great Plains, USA. *Annals of Botany* 127(4): 451-459 (2021). https://doi.org/10.1093/aob/mcaa146
24. L. Lombardini and L. Rossi. Ecophysiology of plants in dry environments. In: Dryland Ecohydrology. P. D'Odorico, A. Porporato, and C.W. Runyan (Eds.). *Springer, Cham, Switzerland* pp. 71-100 (2019). https://doi.org/10.1007/978-3-030-23269-6_4
25. J. Kociecka, D. Liberacki, and M. Stróżecki. The role of antitranspirants in mitigating drought stress in plants of the grass family (Poaceae)—A Review. *Sustainability* 15(12): 9165 (2023). https://doi.org/10.3390/su15129165
26. M.S. Hassan, N. Naz, H.R. Javeed, S. Zafar, L. Kanwal, S. Mariyum, A. Fatima, A. Bashir, and M.I. Atta. Biodiversity Assessment of Weed Communities in Tube-Well Irrigated Wheat Fields in District Layyah, Punjab, Pakistan. *Pakistan Journal of Weed Science Research* 30(2): 55-64 (2024). https://doi.org/10.17582/journal.PJWSR/2024/30.2.55.64
27. M. Majeed, K.H. Bhatti, M.S. Amjad, A.M. Abbasi, R.W. Bussmann, F. Nawaz, A. Rashid, A. Mehmood, M. Mahmood, and W.M. Khan. Ethno-veterinary uses of Poaceae in Punjab, Pakistan. *PLoS One* 15(11): e0241705 (2020). https://doi.org/10.1371/journal.pone.0241705
28. J. Pardo and R. VanBuren. Evolutionary innovations driving abiotic stress tolerance in C4 grasses and cereals. *The Plant Cell* 33(11): 3391-3401 (2021). https://doi.org/10.1093/plcell/koab205
29. S. Ahmad, M. Zafar, M. Ahmad, M.I. Ali, S. Sultana, N. Rashid, M.A. Butt, S.N. Shah, F.A. Ozdemir, M.A. Kutlu, R. Afza, A. Usma, and M. Nazish. Seed morphology using SEM techniques for identification of useful grasses in Dera Ghazi Khan, Pakistan. *Microscopy Research and Technique* 83(3): 249-258 (2020). https://doi.org/10.1002/jemt.23408
30. B. Sadia, M. Ahmad, A.A. Alsahli, Z.K. Shinwari, S. Khawaja, B. Avutkhanov, S. Sultana, and W. Noor. Taxonomic and ecological implications of culm histology in family Poaceae. *Pakistan Journal of Botany* 57(3): 1101-1115 (2025). https://doi.org/10.30848/PJB2025-3(25)
31. B. Sadia, M. Ahmad, W. Noor, S.W. Gillani, M. Manzoor, Z. Chen, L. Zhang, S. Sultana, and A. Sohail. Morpho-palynological evaluation of family Poaceae from arid and semi-arid regions of Pakistan. *Genetic Resources and Crop Evolution* 72(8): 9763-9790 (2025). https://doi.org/10.1007/s10722-025-02527-4
32. Y. Ali, S. Iqbal, H.M. Aatif, K. Naveed, A.A. Khan, M. Ijaz, M.M. Magsi, S. Ahmad, A.U.A. Syed, M.A. Magsi, R.K. Iqbal, and A. Raza. Environmental-responses based predictive modelling for stripe rust severity in wheat by using meteorological data from Layyah. *Journal of King Saud University - Science* 35(2): 102591 (2023). https://doi.org/10.1016/j.jksus.2023.102591
33. D.L. Dilcher. Approaches to the identification of angiosperm leaf remains. *The Botanical Review* 40(1): 1-157 (1974). https://www.jstor.org/stable/i398083
34. S.N. Shah, M. Ahmad, M. Zafar, K. Malik, N. Rashid, F. Ullah, and S. Sultana. A light and scanning electron microscopic diagnosis of leaf epidermal morphology and its systematic implications in Dryopteridaceae: Investigating 12

ACCEPTED MANUSCRIPT

Pakistani taxa. *Micron* 111: 36-49 (2018). https://doi.org/10.1016/j.micron.2018.05.008

35. M. Nazish, M. Ahmad, R. Ullah, A.A. Shahat, D. Potter, M. Zafar, and S. Sultana. Taxonomic implications of leaf epidermis in halophytes of Amaranthaceae from Salt Range of Punjab, Pakistan. *Plant Biosystems* 156(1): 79-90 (2022). https://doi.org/10.1080/11263504.2020.1837277
36. C.R. Metcalfe. Anatomy of the Monocotyledons. I. Gramineae. *Clarendon Press, Oxford, UK* (1960).
37. C.R. Metcalfe. Anatomy of the Monocotyledons. V. Cyperaceae. *Clarendon Press, Oxford, UK* (1971).
38. F. Hadi, S. Dost, M.N. Khan, B. Ullah, A. Razzaq, K. Hayat, A. Kaplan, M. Iqbal, S.N. Shah, S. Wahab, F.R. Butt, S.A. Razak, S. Ercisli, M.A. Ali, and J. Alkahtani. Foliar LM and SEM insights: Investigating epidermal features and its taxonomic implications in some Verbenaceae taxa. *Polish Journal of Environmental Studies* 34(3): 2673-2685 (2025). https://doi.org/10.15244/pjoes/188235
39. M. Manzoor, M. Ahmad, S.W. Gillani, M. Zafar, J. Hussain, M.K.A. Ansari, H. Rizwana, I. Abid, M. Imran, and S. Jabeen. Micromorphological and ultrastructural exploration of *Sorbus foliolosa* (Rosaceae) populations from the Himalayan region of Kashmir. *Polish Journal of Environmental Studies* 34(4): 4765-4774 (2025). https://doi.org/10.15244/pjoes/190597
40. W. Noor, M. Zafar, M. Ahmad, B. Sadia, S.W. Gillani, M. Manzoor, and M. Ameen. Taxonomic significance of palyno-morphic markers for the delimitation of some Brassicaceous taxa in Balochistan Province (Pakistan). *Genetic Resources and Crop Evolution* 72(1): 587-614 (2025). https://doi.org/10.1007/s10722-024-01997-2
41. S.S. Tassadduq, S. Akhtar, M. Waheed, N. Bangash, D. Nayab, M. Majeed, S. Abbasi, M. Muhammad, A. Alataway, A.Z. Dewidar, H.O. Elansary, and K. Yessoufou. Ecological distribution patterns of wild grasses and abiotic factors. *Sustainability* 14(18): 11117 (2022). https://doi.org/10.3390/su141811117
42. G. Lino, P. Espigul, S. Nogués, and X. Serrat. *Arundo donax* L. growth potential under different abiotic stress. *Heliyon* 9(5): e15521 (2023). https://doi.org/10.1016/j.heliyon.2023.e15521
43. E. Sánchez, P. Rivera-Vargas, X. Serrat, and S. Nogués. *Arundo donax* L.: how high photosynthetic capacity is kept under water scarcity conditions. *Agronomy* 11(6): 1089 (2021). https://doi.org/10.3390/agronomy11061089
44. J.A. Bushey, A.M. Hoffman, S.M. Gleason, M.D. Smith, and T.W. Ocheltree. Water limitation reveals local adaptation and plasticity in the drought tolerance strategies of *Bouteloua gracilis*. *Ecosphere* 14(1): e4335 (2023). https://doi.org/10.1002/ecs2.4335
45. S. Pierce, R.M. Ceriani, R. De Andreis, A. Luzzaro, and B. Cerabolini. The leaf economics spectrum of Poaceae reflects variation in survival strategies. *Plant Biosystems* 141(3): 337-343 (2007). https://doi.org/10.1080/11263500701627695
46. F. Fort, C. Jouany, and P. Cruz. Root and leaf functional trait relations in Poaceae species: Implications of differing resource-acquisition strategies. *Journal of Plant Ecology* 6(3): 211-219 (2013). https://doi.org/10.1093/jpe/rts034
47. A.E. Carmo-Silva, A. Francisco, S.J. Powers, A.J. Keys, L. Ascensão, M.A.J. Parry, and M.C. Arrabaça. Grasses of different C4 subtypes reveal leaf traits related to drought tolerance in their natural habitats: Changes in structure, water potential, and amino acid content. *American Journal of Botany* 96(7): 1222-1235 (2009). https://doi.org/10.3732/ajb.0800224
48. L. Chen and R. Wang. Anatomical and physiological divergences and compensatory effects in two *Leymus chinensis* (Poaceae) ecotypes in Northeast China. *Agriculture, Ecosystems & Environment* 134(1-2): 46-52 (2009). https://doi.org/10.1016/j.agee.2009.05.015
49. Z.J. Guan, S.B. Zhang, K.Y. Guan, S.Y. Li, and H. Hu. Leaf anatomical structures of *Paphiopedilum* and *Cypripedium* and their adaptive significance. *Journal of Plant Research* 124(2): 289-298 (2011). https://doi.org/10.1007/s10265-010-0372-z
50. B. Li, Y. Chen, D. Wang, Y. Xue, M. Qu, S. Shao, S. Nie, and J. Li. Leaf anatomical structure of dominant shrubs and their influencing factors across habitats in hyper-arid region. *Chinese Journal of Applied Ecology* 36(8): 2370-2378 (2025). https://doi.org/10.13287/j.1001-9332.202508.010
51. K. Ozeki, Y. Miyazawa, and D. Sugiura. Rapid stomatal closure contributes to higher water use efficiency in major C4 compared to C3 Poaceae crops. *Plant Physiology* 189(1): 188-203 (2022). https://doi.org/10.1093/plphys/kiac040
52. T. Yamauchi, O. Pedersen, M. Nakazono, and N. Tsutsumi. Key root traits of Poaceae for adaptation to soil water gradients. *New Phytologist* 229(6): 3133-3140 (2021). https://doi.org/10.1111/nph.17093
53. A.M. Zuffo, F. Steiner, J.G. Aguilera, R.F. Ratke, L.M. Barrozo, R. Mezzomo, A.S. dos Santos, H.H.S. Gonzales, P.A. Cubillas, and S.M. Ancca. Selected indices to find water-stress-tolerant tropical forage

ACCEPTED MANUSCRIPT

grasses. *Plants* 11(18): 2444 (2022). https://doi.org/10.3390/plants11182444

54. J.T. Olsen, K.L. Caudle, L.C. Johnson, S.G. Baer, and B.R. Maricle. Environmental and genetic variation in leaf anatomy among populations of *Andropogon gerardii* (Poaceae) along a precipitation gradient. *American Journal of Botany* 100(10): 1957-1968 (2013). https://doi.org/10.3732/ajb.1200628
55. N. Kabir, S. Wahid, S.U. Rehman, and G. Qanmber. The intricate world of trichome development: From signaling pathways to transcriptional regulation. *Environmental and Experimental Botany* 217: 105549 (2024). https://doi.org/10.1016/j.envexpbot.2023.105549
56. H. Singh, N. Kumar, and A. Kumar. Enhancing resource use efficiency in crops through plant functional traits. In: Plant Functional Traits for Improving Productivity. N. Kumar and H. Singh (Eds.). *Springer*, *Nature, Singapore* pp. 97-117 (2024). https://doi.org/10.1007/978-981-97-1510-7_6
57. N. He, G. Yu, C. Liu, Y. Li, and R. Wang. Variation, Adaptation, and Optimization Mechanism of Plant Functional Traits at the Organ Level. In: Plant Functional Ecology: From Organ to Ecosystem. *Springer, Nature, Singapore* pp. 33-70 (2025). https://doi.org/10.1007/978-981-96-8264-5_2
58. D. Balakrishnan, N. Bateman, and R.R. Kariyat. Rice physical defenses and their role against insect herbivores. *Planta* 259(5): 110 (2024). https://doi.org/10.1007/s00425-024-04381-7
59. I. Kaur, S. Watts, C. Raya, J. Raya, and R. Kariyat. Surface Warfare: Plant structural defenses challenge caterpillar feeding. In: Caterpillars in the Middle: Tritrophic Interactions in a Changing World. R.J. Marquis and S. Koptur (Eds.). *Springer*, *Cham, Switzerland* pp. 65-92 (2022). https://doi.org/10.1007/978-3-030-86688-4_3
60. C.A.E. Strömberg, R.E. Dunn, C. Crifò, and E.B. Harris. Phytoliths in paleoecology: analytical considerations, current use, and future directions. In: Methods in Paleoecology: Reconstructing Cenozoic Terrestrial Environments and Ecological Communities. D.A. Croft, D.F. Su, and S.W. Simpson (Eds.). *Springer*, *Cham, Switzerland* pp. 235-287 (2018). https://doi.org/10.1007/978-3-319-94265-0_12
61. P.-A. Christin and C.P. Osborne. The evolutionary ecology of C4 plants. *New Phytologist* 204(4): 765-781 (2014). https://doi.org/10.1111/nph.13033
62. D.R. Malaviya, A.K. Roy, and P. Kaushal. Comparative leaf anatomical studies reveal photosynthetic pathways type in guinea grass (*Panicum maximum* Jacq.) accessions and their interspecific lineage. *Current Science* 119(5): 808-816 (2020). https://doi.org/10.18520/cs/v119/i5/808-816
63. S.M. Zahedi, M. Karimi, A. Venditti, N. Zahra, K.H.M. Siddique, and M. Farooq. Plant adaptation to drought stress: The role of anatomical and morphological characteristics in maintaining the water status. *Journal of Soil Science and Plant Nutrition* 25(1): 409-427 (2025). https://doi.org/10.1007/s42729-024-02141-w
64. H.P. Linder, C.E.R. Lehmann, S. Archibald, C.P. Osborne, and D.M. Richardson. Global grass (Poaceae) success underpinned by traits facilitating colonization, persistence, and habitat transformation. *Biological Reviews* 93(2): 1125-1144 (2018). https://doi.org/10.1111/brv.12388
65. M. Schubert, A.M. Humphreys, C.L. Lindberg, J.C. Preston, and S. Fjellheim. To coldly go where no grass has gone before: a multidisciplinary review of cold adaptation in Poaceae. *Annual Plant Reviews* Online 3(2): 523-562 (2020). https://doi.org/10.1002/9781119312994.apr0739
66. U. Ahmad, M. Hussain, W. Ahmad, J. Javed, Z. Arshad, and Z. Akram. Impact of global climate change on maize (*Zea mays*): physiological responses and modern breeding techniques. *Trends in Biotechnology and Plant Sciences* 2(1): 62-77 (2024). https://doi.org/10.62460/TBPS/2024.010
67. K.B. Abreha, M. Enyew, A.S. Carlsson, R.R. Vetukuri, T. Feyissa, T. Motlhaodi, D. Ng'uni, and M. Geleta. Sorghum in dryland: morphological, physiological, and molecular responses of sorghum under drought stress. *Planta* 255(1): 20 (2022). https://doi.org/10.1007/s00425-021-03799-7
68. Y.-F. Liu, L.-C. Meng, Z. Huang, Z.-H. Shi, and G.-L. Wu. Contribution of fine roots mechanical property of Poaceae grasses to soil erosion resistance on the Loess Plateau. *Geoderma* 426: 116122 (2022). https://doi.org/10.1016/j.geoderma.2022.116122

ACCEPTED MANUSCRIPT